Resonance region to DIS, quark-hadron duality at Jefferson Lab

S. A. Wood[a]

[a]Thomas Jefferson National Accelerator Facility, 12000 Jefferson Avenue,
Newport News, VA 23602, USA

New measurements of inclusive electron scattering on the proton and deuteron have been made at Jefferson Lab with a four-momentum transfer range of $0.3 \leq Q^2 \leq 4.5$ $(\mathrm{GeV}/c)^2$ as a study of quark-hadron duality at low Q^2. The F_2 structure function is found to scale about a common scaling curve down to Q^2 of 0.5 $(\mathrm{GeV}/c)^2$, indicating that higher twist effects are small. Duality in other observables and in electron scattering on nuclei are also discussed.

1. History

The F_2 structure function from deep inelastic electron scattering ((e,e') at $W^2 > 4$ GeV^2) exhibits the logarithmic scaling in x behavior expected from PQCD. For $W^2 < 4$ GeV^2 and Q^2 below a few GeV$/c^2$ this scaling breaks down as the the low lying resonances of the proton become prominent and target mass effects become important.

However, Bloom and Gilman observed [1] that, qualitatively, in the regions of these resonances, the resonance peaks tend to oscillate about the scaling curve from higher Q^2 when the scaling variable $\omega' = 1 + W^2/Q^2$ is used with data in the range $1 \leq Q^2 \leq 10$ $(\mathrm{GeV}/c)^2$. This "duality" between low-energy electro-production of resonances and high energy scattering have traditionally been interpreted to mean that higher-twist effects are not large or at least cancel when one averages over the resonances [2].

Because of advances in the understanding of QCD and improvements in F_2 measurements in deep inelastic scattering (DIS), quark-hadron duality is becoming more quantitative. Jefferson Lab has undertaken a program of measurements in the resonance region of F_2 and other observables over a wide Q^2 range with an emphasis on very low Q^2 measurements.

2. Jefferson Lab Results

Inelastic $p(e,e')$ measurements were made in Hall C at Jefferson Lab using the HMS spectrometer [3,4]. Electron beams of 2.45 to 4.05 GeV$/c$ were scattered off of 4 cm LH_2 and LD_2 targets with scattering angles ranging from 20 to 70 degrees. At each beam energy/scattering angle combination, measurements were made at a series of overlapping momentum bites ranging from the elastic peak down to a scattering energy that corresponds to $W^2 \approx 5$ GeV^2.

As double differential cross sections are continuum measurements, attention to backgrounds is important. Pion production, (e^-,π^-), at deeply inelastic momenta can exceed (e,e') by as much as a factor of 10. Electrons are identified by requiring a signal in a gas Cerenkov detector and a large signal from an electromagetic shower in a lead glass detector. The combination of these two detectors can reject pions at a factor of about 1000:1. Another significant background for deeply inelastic scattering is electrons from e^+e^- pair production. This background is removed by using calculations and verifying those calculations with measurements of inclusive (e^-,e^+) made at the same kinematics as the (e,e') measurements.

Proper handling of radiative corrections is also important for electron scattering to the continuum. Radiation of photons by either the electron or the target has the effect of making the $(\vec{q},\omega)$ of the exchange photon different from that calcu-

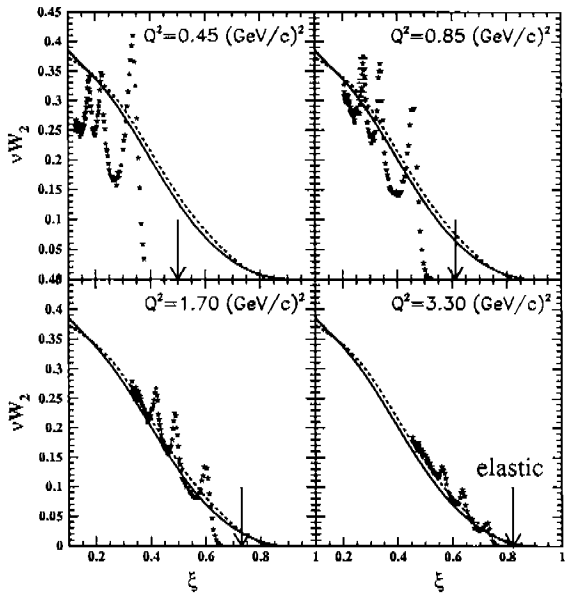

Figure 1. F_2 from JLab $p(e,e')$ data (stars) compared to the NMC [7] parameterization evaluated at $Q^2 = 5$ (GeV/c)^2 (dashed line) and $Q^2 = 10$ (GeV/c)^2 (solid line). Arrows indicate elastic kinematics.

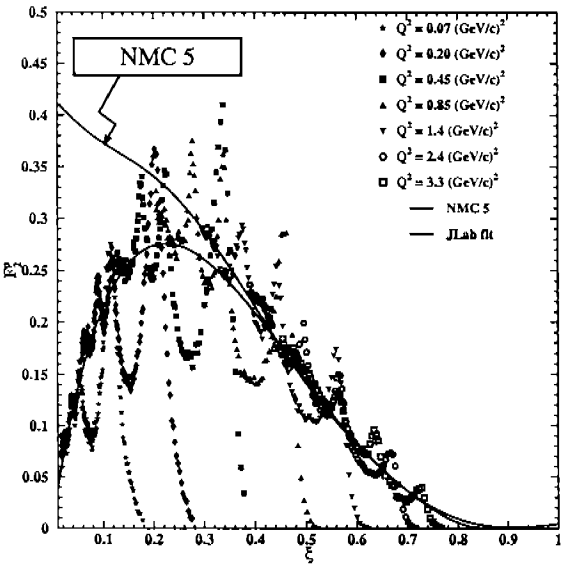

Figure 2. JLab hydrogen F_2 data including low Q^2 measurements. The solid curves are the NMC parameterization for a fixed $Q^2 = 5$ (GeV/c)^2 and the the JLab fit (Eqn. 2).

lated from beam energy and the observed scattered electron momentum vector. An example of an important radiative effect is the radiation of a photon by the incoming electron. Through this, elastic scattering at lower incoming electron electron energies, where cross sections are higher, can appear at high w in the energy loss spectra from higher beam energies. To correct for these radiative effects, a good knowledge of the same cross section that is being measured is required, thus an iterative procedure is used to unfold radiative and other effects.

The measured cross section is a linear combination of two structure functions. The structure function F_2 is extracted from the cross section using

$$\frac{\sigma \nu Q^2}{4\alpha^2 E'^2} = F_2 \left[\cos^2\left(\frac{\theta}{2}\right) + 2\sin^2\left(\frac{\theta}{2}\right) \frac{1+\nu^2/Q^2}{R+1} \right], \qquad (1)$$

where $R = \sigma_L/\sigma_T$ is the ratio of the longitudinal to the transverse cross sections. While the uncertainties in R are large for the kinematics measured here, they only contribute a 2% systematic uncertainty to F_2. (More precise measurements of R, discussed below, are underway at JLab [5].) Overall, the systematic errors in F_2 due to uncertainty in R, radiative corrections, pair production, backgrounds and other experimental effects total about 3.5%. Statistical errors are approximately 1%.

3. Results and Discussion of Data

A sample of the $p(e,e')$ F_2 results are shown in Fig. 1, plotted as a function of the Nachtmann scaling variable $\xi = 2x/(1+\sqrt{1+4x^2M^2/Q^2})$ which is the proper scaling variable to use when studying QCD scaling violations [2,6]. (ξ is very similar to the inverse of the scaling variable ω'

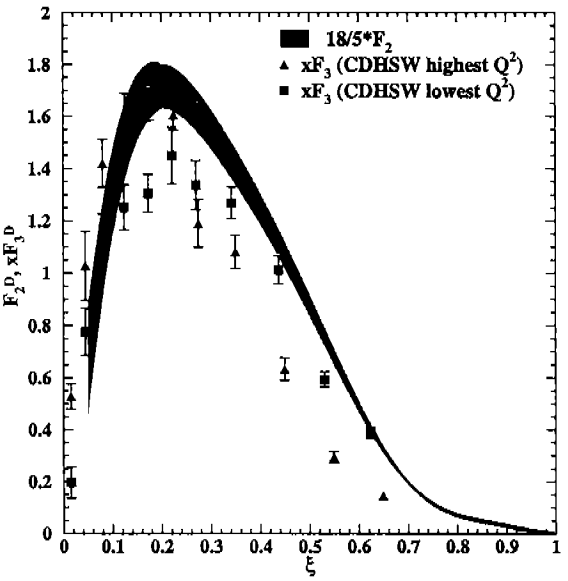

Figure 3. Comparison of of JLab F_2^d data averaged over Q^2 (shaded band) to neutrino scattering measurements of xF_3 [8].

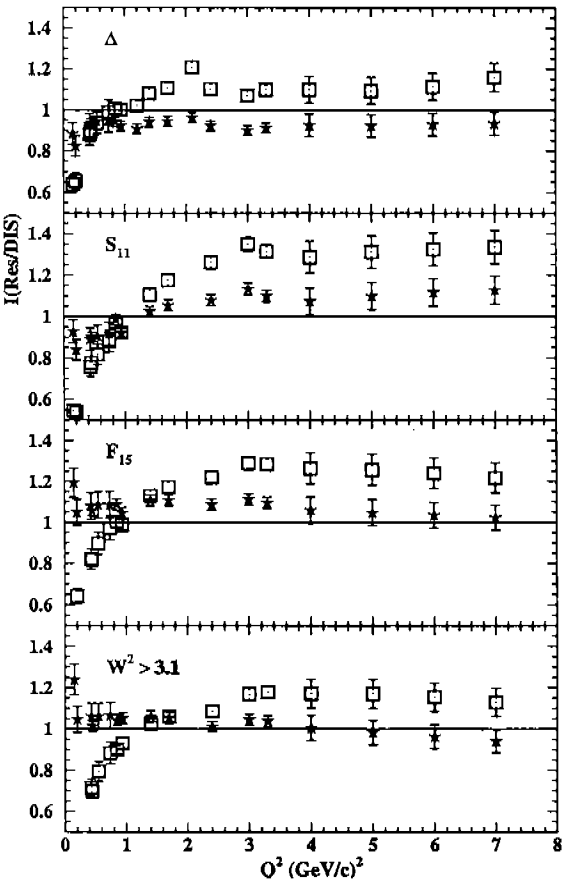

Figure 4. Integral of F_2 data over resonance defined ξ ranges divided by integrals of JLab fit (stars) and NMC (squares) over the same ξ range.

used by Bloom and Gilman). Also shown are curves of the NMC fit [7] to deep inelastic scattering that have been evaluated at $Q^2 = 5$ and 10 $(\mathrm{GeV}/c)^2$. While at different Q^2, the nucleon resonances appear at different ranges of ξ, the NMC fit is generally the average of the data, confirming the original Bloom and Gilman observations. This suggests that, in the Operator Product Expansion [2], higher twist effects are small, at least on average, at these low Q^2 kinematics.

The NMC fit continues to rise as it is extended to lower ξ. However, below $\xi = 0.3$, the JLab resonance region F_2 starts to deviate from NMC. The average shape described by the low ξ resonance data (which are at low Q^2) (Fig. 2) is reminiscent of quark distributions from valence quarks only.

This valence like behavior can be explored by comparing electron scattering data with xF_3 from deep inelastic neutrino-iron scattering [8,9]. xF_3 measures the difference between quark and antiquark distributions and is in first order not sensitive to sea quarks. In Fig. 3, the neutrino xF_3 measurements are compared to the F_2 measurements on deuterium. The deuterium F_2 data has been averaged over all the Q^2 values of the JLab data set and is represented by the shaded band. The deuterium F_2 data and the iron xF_3 data have been scaled by straight forward factors to account for the quark charges in deuterium and the A of iron. The similarity in the distributions suggests that low Q^2 electron scattering may be a method of accessing valence quark distributions at low x.

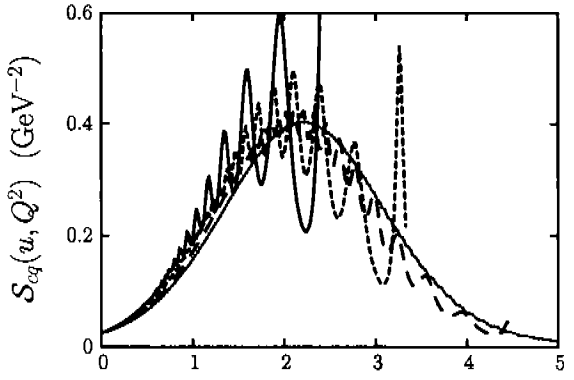

Figure 5. Simple nucleon model [10] showing onset of scaling of structure function S_{cq} vs u, a Nachtmann-type scaling variable. Successively smoother curves a fore $Q^2 = 0.5, 1, 2,$ and5 (GeV$/c)^2$.

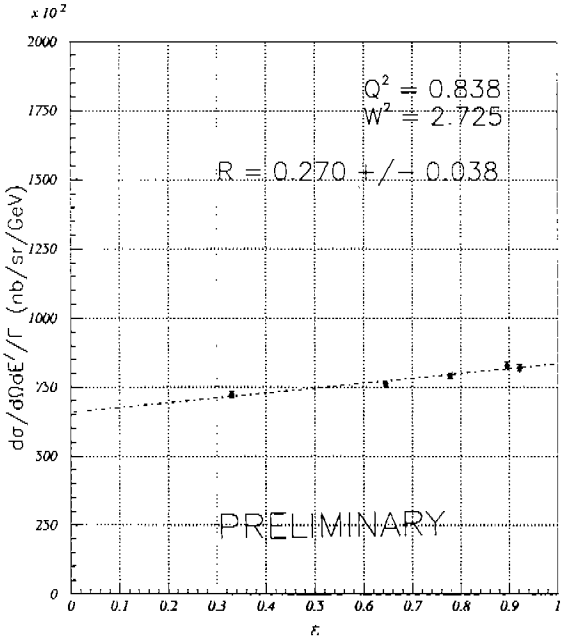

Figure 6. Example of extraction of R by measuring slope of cross section as a function of $\epsilon = [1 + 2(1 + \nu^2/Q^2)\tan^2(\theta/2)]^{-1}$

Because the low ξ data appear, on average, to follow a common curve that differs from the NMC parameterization, an average scaling curve using only hydrogen resonance data has been obtained. The entire Q^2 and W^2 range of the F_2 data was fit to a functional form that depends *only* on ξ. This JLab duality fit,

$$\begin{aligned} F_2 &= \xi^{0.870}(1-\xi)^{0.006} \\ &\times[0.005 - 0.058(1-\xi) - 0.017(1-\xi)^2 \\ &+ 2.469(1-\xi)^3 - 0.240(1-\xi)^4], \end{aligned} \quad (2)$$

is shown with the data in Fig. 2.

The effect of resonances on duality can be more quantitatively investigated by comparing F_2 in the regions of the prominent resonances to various scaling curves. To delimit the prominent resonances, we choose the following ranges of W^2: $\Delta(1.3 \leq W^2 < 1.9$ GeV$^2)$, $S_{11}(1.9 \leq W^2 < 2.5$ GeV$^2)$, $F_{15}(2.5 \leq W^2 < 3.1$ GeV$^2)$, and $(3.1 \leq W^2 < 3.9$ GeV$^2)$. To compare the resonance data to DIS or the JLab duality fit, F_2 resonance data for a given Q^2 is integrated over a range of ξ that corresponds to the W^2 range of the resonance. This integral is divided by the integral of the DIS or duality curve F_2 over the same range. (The ξ range will be different for each value of Q^2 at which the ratio is evaluated).

$$I(res/\mathrm{DIS}) = \frac{\int_{\xi_a}^{\xi_b} F_2{}^{\mathrm{data}}}{\int_{\xi_a}^{\xi_b} F_2{}^{\mathrm{scaling}}}. \quad (3)$$

This ratio of resonance data to both the NMC parameterization and the JLab fit is shown in Fig. 4. For the NMC comparison, the ratio exceeds one for most of the Q^2 range, but by a roughly constant amount over Q^2 and for all the resonance regions. For $Q^2 < 3$(GeV$/c)^2$ the ratio is no longer constant, dropping below one. This is a manifestation of the valence like behavior exhibited in our measurements of F_2 and the fact that at low Q^2, the resonances appear at low values of ξ. When the JLab resonance fit is used instead, the ratio is generally within 10% of unity. While this is a ratio between data and a fit to the same data, which thus includes the valence-like behavior, it is worth reiterating that the JLab fit depends only

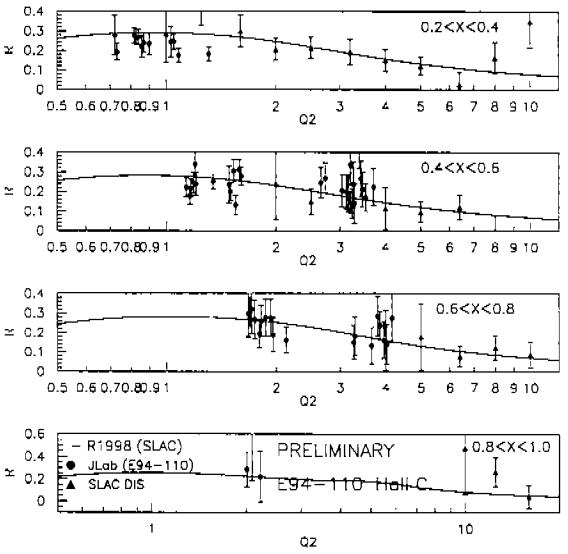

Figure 7. Measurements and fits to R (σ_L/σ_T). Triangles: SLAC R data for DIS region ($W^2 > 3$ GeV^2) [11]; Circles: JLab R data for nucleon resonance region; Line: SLAC global fit (R1998) [12] to DIS data.

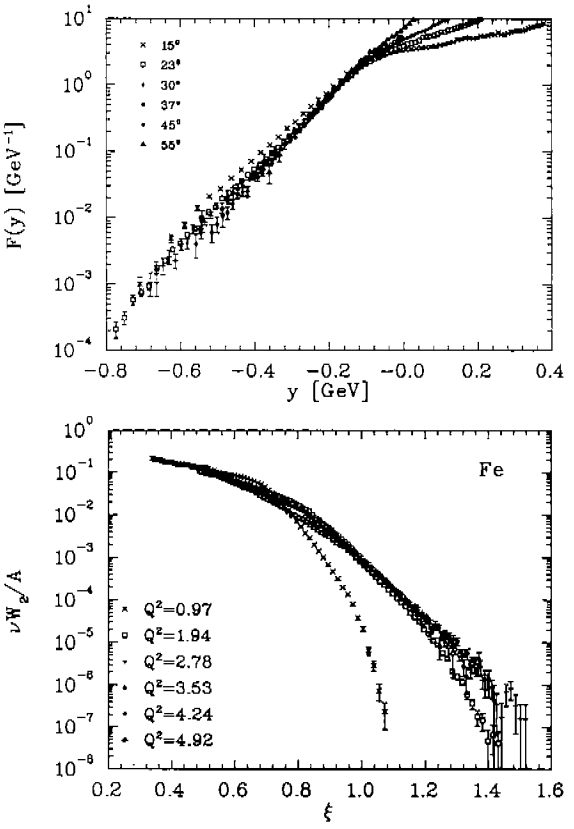

Figure 8. JLab ^{56}Fe(e,e') data. Top: $F(y)$ scaling function; Bottom: F_2/A vs. ξ for same data

on ξ and thus has no Q^2 dependence.

In a recent theoretical discussion of duality [10], a simple nucleon model consisting of two scaler quarks, one of which is heavy, is considered. This model has no continuum, only a spectrum of resonances that are given small arbitrary widths. In this model, duality is observed between the low Q^2 spectra where resonances dominate and higher Q^2 where the spectra are smooth. (Fig. 5). An important implication of this work is that the distinction between resonance region scattering and deep inelastic scattering at higher W^2 is artificial. As Q^2 is increased, the increasing density of resonances (in the scaling variable) simply serves to mimic a continuum.

4. Duality in R and Nuclei

Duality is also being explored in measurements of R. R is the ratio of the longitudinal to transverse inelastic electron scattering cross sections. By measuring F_2 and R, unpolarized electron scattering is fully described. The electron scattering cross section can be written as:

$$\frac{d^2\sigma}{d\Omega d\nu} = \Gamma[\sigma_T(W^2,Q^2) + \epsilon\sigma_L(W^2,Q^2)], \qquad (4)$$

where $\epsilon = [1 + 2(1+\nu^2/Q^2)\tan^2(\theta/2)]^{-1}$, and Γ, the transverse virtual photon flux, is a function of kinematic quantities. R is then extracted by making measurements of the cross section at several scattering angles, (but with fixed W^2 and Q^2), and observing the slope of σ/Γ as a function of ϵ. (See Fig. 6).

Measurements of R are being made at JLab over the same kinematic range as the measure-

ments of F_2. Preliminary values for R are compared to SLAC data [11] in Fig. 7. The SLAC data shown are deep inelastic scattering kinematics, ($W^2 > 3$ GeV^2), compared to the JLab data which are obtained at resonance kinematics. The low Q^2 measurements of R connect smoothly to the higher Q^2 DIS measurements for a broad range of x indicating the validity of duality for this observable.

Inclusive electron scattering measurements are also being carried out on nuclei [13]. For the momentum transfer range studied (1 (GeV/c)^2 $< Q^2 < 6$ (GeV/c)^2), such measurements are generally analyzed as scattering off of bound nucleons. By dividing $A(e,e')$ cross sections by off-shell electron-nucleon cross sections (σ_p and σ_n), a scaling function can be defined:

$$F(y) = \frac{d^2\sigma}{d\Omega d\nu} \frac{1}{Z\sigma_p + N\sigma_n} \frac{q}{\sqrt{M^2 + (y+q)^2}}, \quad (5)$$

where y is defined by $\nu + M_A = (M^2 + q^2 + y^2 + 2yq)^{1/2} + (M_{A-1}^2 + y^2)^{1/2}$. With this scaling function, the $Fe^{56}(e,e')$ data scale well for negative y. (Fig. 8 top) Large negative y corresponds to kinematics where the "initial struck nucleon" has a high momentum. However, for $y = 0$ and positive, which correspond to quasi-free scattering and deep inelastic scattering, this scaling breaks down.

The success of the duality approach on free nucleons suggests analyzing inclusive electron scattering on nuclei as electron-quark scattering using the variable ξ as the scaling variable. When the F_2 structure function per nucleon is evaluate as in Eqn. 1, the iron data are found to scale (Fig. 8 bottom) for a large range of ξ over which the structure function varies by six orders of magnitude [14]. For $\xi < 1$ this scaling is perhaps not surprising as the Fermi motion of nucleons in the nucleus supplies the "averaging" needed for duality scaling. But it is also interesting that this scaling works for $\xi > 1$ (and thus also $x > 1$) for all but the lowest Q^2 data.

$A(e,e')$ measurements have been made on deuterium, C, Fe and Au targets with a 4 GeV/c electron beam. Future measurements [15] will also include ^{4}He and ^{4}He targets and use a 6 GeV/c beam in order to cover a Q^2 range of up to 10 (GeV/c)^2.

5. Further Duality Related Studies at JLab

Jefferson Lab is continuing to pursue a wide variety of duality related structure function measurements. The hydrogen and deuterium F_2 measurements will be pushed to Q^2 as low as 0.03 (GeV/c)^2 and $x < 0.01$ [16]. This will explore the connection between low Q^2 and insensitivity to the quark sea. F_2^p and F_2^d measurements will also be pushed to intermediate Q^2 (up to 7 (GeV/c)^2) while remaining in the resonance region ($W^2 < 4$ GeV^2) [17]. These data will allow using the duality approach to obtain an averaged F_2 behavior at large x. Such measurements will be extended further with the 12 GeV upgrade at JLab.

As well as the unpolarized structure functions, several experiments measuring the spin structure functions g_1 and g_2 have completed data taking. Among these are the Hall C Resonant Spin Structure experiment [18] and the CLAS eg1 experiment [19] which have obtained resonace region data on hydrogen and deuterium for $0.2 < Q^2 < 1.5$ (GeV/c)^2 and $Q^2 = 5$ (GeV/c)^2. Furthermore, an upcoming Hall A experiment [20] will use polarized ^{3}He to extract g_1^n up to $Q^2 = 5.4$ (GeV/c)^2 with resonance region kinematics in order to access high x.

A new area of research at JLab is meson duality. At high energies, $(e,e'$meson) cross sections can be factorized into quark scattering and quark fragmentation pieces. Work at Cornell [21] and preliminary studies at JLab suggests that factorization and an approximate duality may work at $Q^2 < 3$ (GeV/c)^2 and in the resonance region. These ideas will be tested with $(e,e'\pi)$ and $(e,e'K)$ on p and d targets [22].

In summary, over the next several years, JLab will build up a broad collection of measurements at low to moderate Q^2 of F_2, R, and g_1 for light nuclei and F_2 and R for heavier nuclei. In addition, a program of studying duality in meson production and testing factorization at low energies will be started.

6. Acknowledgements

The author thanks C. Keppel, R. Ent and the F_2, R and $x > 1$ collaborations. This work was supported by DOE Contract No. DE-AC05-84ER40150 under which the Southeastern Universities Research Association (SURA) operates the Thomas Jefferson National Accelerator Facility (Jefferson Lab).

REFERENCES

1. E. D. Bloom and F. J. Gilman, Phys. Rev. Lett. **25**, 1140 (1970); Phys. Rev. D **4**, 2901 (1971).
2. A. De Rujula, H. Georgi, and H. D. Politzer,
3. I. Niculescu *et al.*, Phys. Rev. Lett. **85**, 1186 (2000).
4. I. Niculescu *et al.*, Phys. Rev. Lett. **85**, 1182 (2000).
5. Jefferson Lab Experiment E94-110. Ann. Phys. **103**, 315 (1977); H. Georgi and H. D. Polizer, Phys. Rev. D **14**, 1829 (1976).
6. O. Nachtmann, Nucl. Phys. **B63**, 237 (1975).
7. M. Arneodo *et al.*, Phys. Lett. B **364**, 107 (1005); **364**, 295 (1984).
8. P. Berge *et al.*, Z. Phys. C **49**, 187 (1991).
9. E. Oltman *et al.*, Z. Phys. C **53**, 51 (1992); J. H. Kim *et al.*, Phys. Rev. Lett. **81**, 3595 (1998).
10. N. Isgur *et al.*, Phys. Rev. D **64**, 054005 (2001).
11. S. Dasu *et al.*, Phys. Rev. Lett. **61**, 1061 (1988); Phys. Rev. D **49**, 5641 (1994); L. Whitlow *et al.*, Phys. Lett. B **250**, 193 (1990); L. H. Tao *et al.*, Z. Phys. C **70**, 387 (1996).
12. K. Abe *et al.*, Phys. Lett. B **452**, 194 (1999).
13. J. Arrington *et al.*, Phys. Rev. Lett. **82**, 2056 (1999).
14. J. Arrington *et al.*, Phys. Rev. C **64**, 014602 (2001).
15. J. Arrington, D. Day, B. Filippone, and A. Lung, Jefferson Lab Experiment E02-019.
16. Jefferson Lab experiment E00-002.
17. Jefferson Lab experiment E00-116.
18. Jefferson Lab experiment E01-006.
19. T. A. Forest and the CLAS collaboration, talk presented at the 9th International Conference on the Structure of Baryons, Jefferson Lab, 2002.
20. Jefferson Lab experiment E01-012.
21. Bebek *et al.*, Phys. Rev. Lett. **34**, 75 (1975); Phys. Rev. Lett. **37**, 1525 (1976); Phys. Rev. D **15**, 3085 (1977).
22. Jefferson Lab experiment E00-108.